arXiv:nucl-th/0607017v1 10 Jul 2006

Partial-Wave Analysis of Single-Pion Production Reactions

R.A. Arndt*, W.J. Briscoe*, I.I. Strakovsky* and R.L. Workman*

*Center for Nuclear Studies, Department of Physics, The George Washington University, Washington, D.C. 20052, USA

Abstract. We present an overview of our efforts to analyze pion-nucleon elastic scattering data, along with data from related photo- and electroproduction reactions, in order to study the baryon spectrum. We then focus on the $\Delta(1232)$ resonance. Fits to pion photo- and electroproduction data have been used to extract values for the R_{EM} = E2/M1 and R_{SM} = S2/M1 ratios as functions of Q^2. These results are compared to other recent determinations.

Keywords: Partial-Wave Analysis
PACS: 14.20.Gk, 11.80.Et, 13.30.Eg

Many of our fits to scattering data have been motivated by ongoing studies of the N^* properties [1]. Most of these require, as input, amplitudes extracted from elastic pion-nucleon scattering data [2]. Our pion photoproduction multipoles

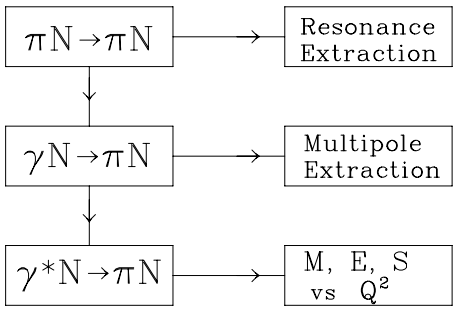

FIGURE 1. Δ multipoles from analysis of scattering data − a Road Map.

are determined using a K-matrix formalism, based upon pion-nucleon partial-wave amplitudes [3]. The electroproduction analysis is similarly anchored to our $Q^2 = 0$ photoproduction results, with additional factors intended to account for the Q^2 variation. This relationship is diagrammed in Fig. 1. Most of what we discuss here is confined to an energy region covering the $\Delta(1232)$ resonance. Problems associated with the opening of channels beyond πN [4] are avoided.

The pion-nucleon amplitudes are determined through a fit to elastic scattering, charge-exchange, and ηN production data, constrained to satisfy forward and fixed-t dispersion relations. A flowchart for this procedure is given in Fig. 2. Two representative results for the partial-wave amplitudes are given in Fig. 3, which shows that the extraction of resonance contributions is difficult for most states. A search of the complex energy plane finds poles which are often far from the physical axis, as shown in Fig. 4, making a simple Breit-Wigner parametrization

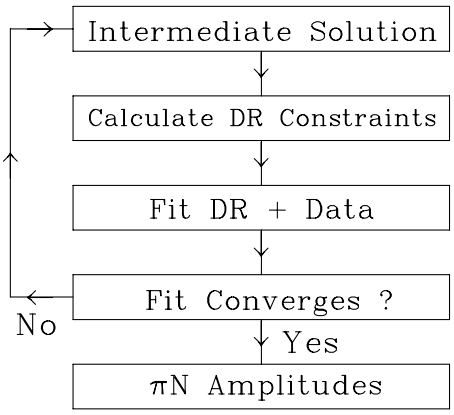

FIGURE 2. πN analysis flow chart.

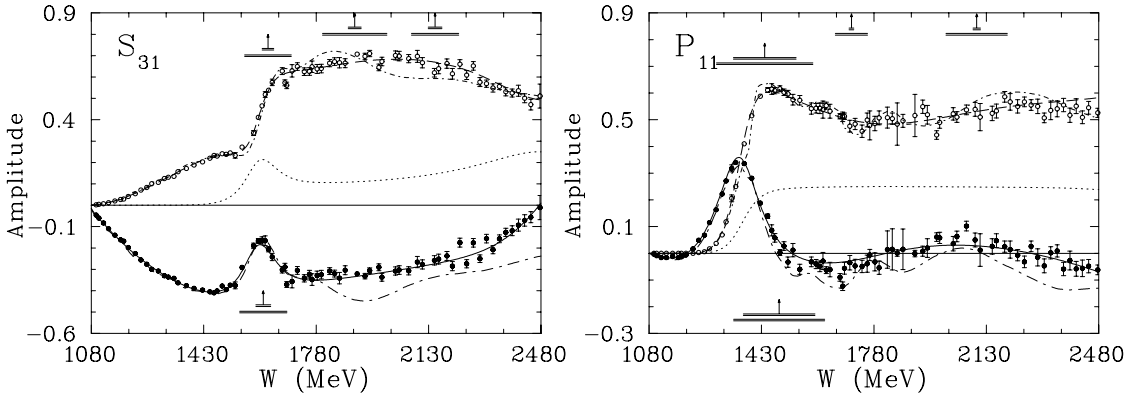

FIGURE 3. Partial-wave amplitudes S_{31} and P_{11} from $T_\pi = 0$ to 2.6 GeV. Solid (dashed) curves give the real (imaginary) parts of amplitudes corresponding to the SP06 solution [2]. The real (imaginary) parts of single-energy solutions are plotted as filled (open) circles. The dotted curve gives the unitarity limit ($ImT - T^*T$) from SP06. The Karlsruhe KA84 solution [5] is plotted with long dash-dotted (real part) and short dash-dotted (imaginary part) lines. All amplitudes are dimensionless. Vertical arrows indicate resonance W_R values and horizontal bars show full Γ and partial $\Gamma_{\pi N}$ widths. The lower BW resonance symbols are associated with the SP06 values; upper symbols give RPP [1] values.

questionable. For the $\Delta(1232)$, however, there is general agreement about the resonance width, mass, pole position, and residue [1]. Here, as the P_{33} partial wave is elastic, a Breit-Wigner fit accurately describes the results of our more involved analysis.

As mentioned, in fitting the electroproduction database, we fix the $Q^2 = 0$ point based on our fits to pion photoproduction. The photoproduction multipoles can be parametrized using the form

$$M = (\text{Born} + \alpha_B)(1 + iT_{\pi N}) + \alpha_R T_{\pi N} + \text{higher terms}, \tag{1}$$

containing the Born terms and phenomenological pieces (α) maintaining the correct threshold behavior and Watson's theorem below the two-pion production

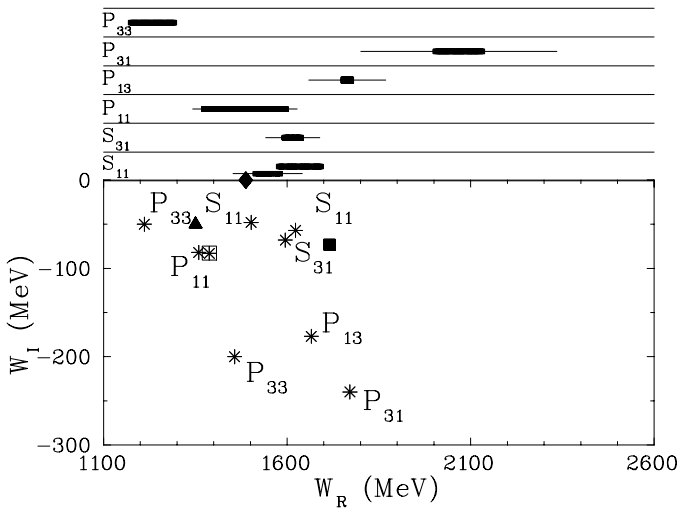

FIGURE 4. Comparison of complex plane (bottom panel) and Breit-Wigner (top panel) parameters for resonances found in the SP06 solution [2]. Plotted are the result for S- and P-wave resonances. Complex plane poles are shown as stars (the boxed star denotes a second-sheet pole). W_R and W_I give real and imaginary parts of the center-of-mass energy. The full (πN partial) widths are denoted by thin (thick) bars for each resonance. The branch point for $\pi\Delta(1232)$, 1350 - i50 MeV, is represented as a solid triangle. The branch points for ηN, 1487 -i0 MeV, and ρN, 1715 - i73 MeV, thresholds are shown as a solid diamond and solid square, respectively.

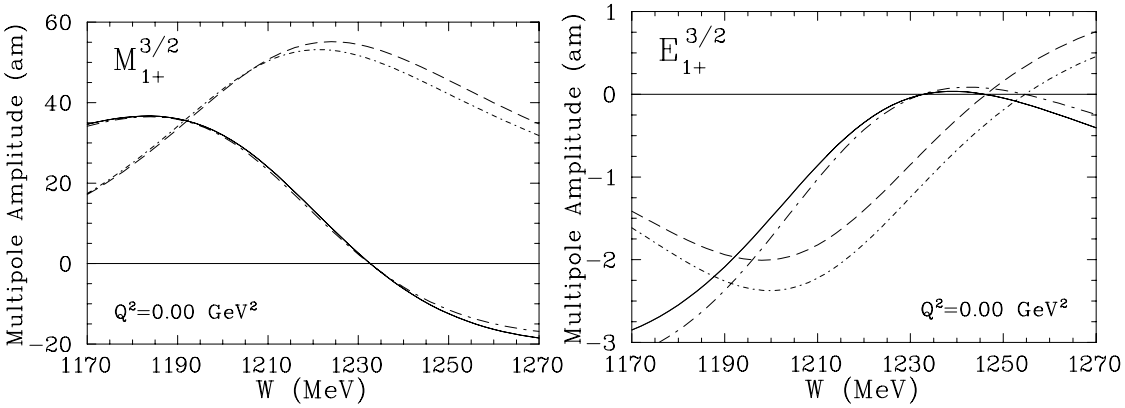

FIGURE 5. Partial-wave P_{33} amplitudes around the $\Delta(1232)$ for $Q^2 = 0.00\ GeV^2$. Magnetic ($M_{1+}^{3/2}$) and electric ($E_{1+}^{3/2}$) multipoles. Solid (dashed) curves give the real (imaginary) parts of amplitudes corresponding to the pion phoproduction SP06 solution [3]. The MAID05 solution [6] is plotted with long dash-dotted (real part) and short dash-dotted (imaginary part) lines.

threshold. The πN T-matrix ($T_{\pi N}$) connects each multipole to structure found in the elastic scattering analysis. In the $\Delta(1232)$ resonance region, the influence of channels beyond πN is small for most partial waves and it is common to drop the α_B and higher order pieces. We retain the α_B term to account for non-pole K-matrix contributions beyond the simple Born terms.

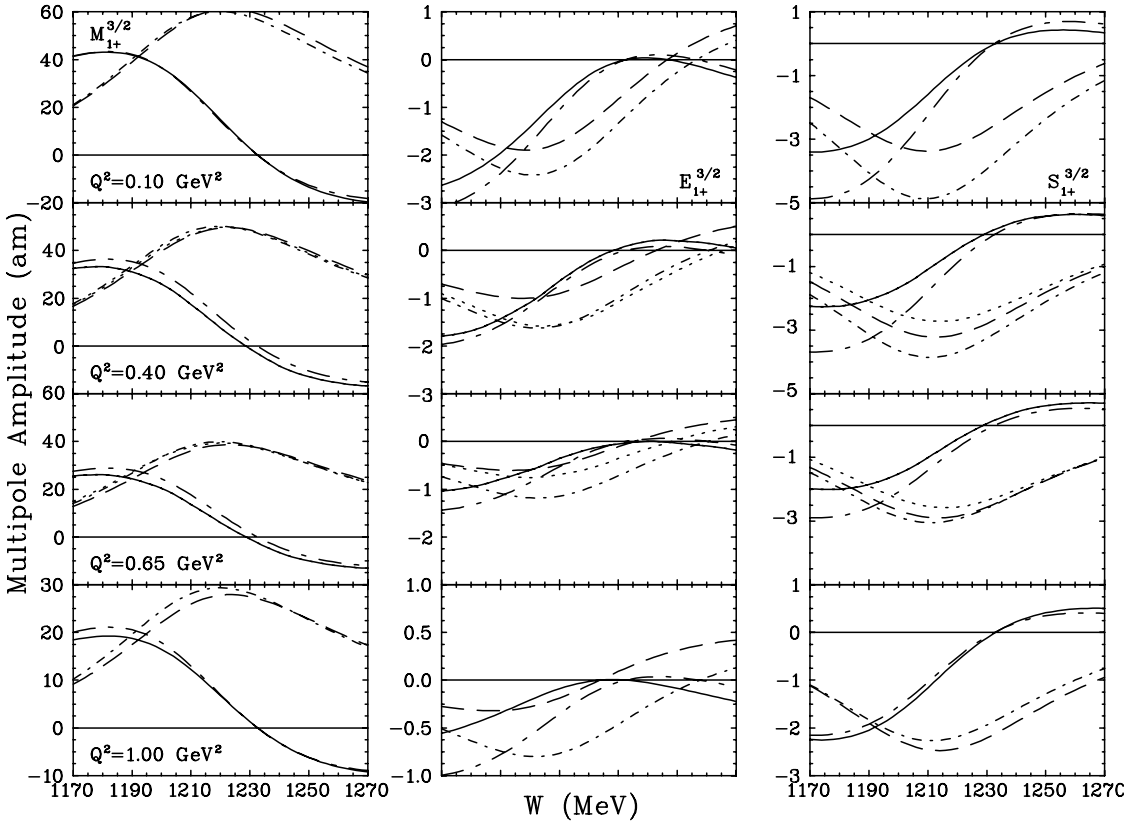

FIGURE 6. Magnetic ($M_{1+}^{3/2}$), electric ($E_{1+}^{3/2}$), and longitudinal ($S_{1+}^{3/2}$) P_{33} multipoles for $Q^2 < 1.50\ GeV^2$. The JM05 results [8] is plotted with dotted (real and imaginary parts) lines for $Q^2 = 0.40$ and $0.65\ GeV^2$. Notation as in Fig. 5.

At non-zero Q^2, the Born terms have built-in Q^2 dependence − other terms have been modified by a phenomenological factor

$$f(Q^2) = \frac{k}{k(Q^2=0)} \frac{1}{1+Q^2/0.7} e^{-\Lambda Q^2} \left(1 + Q^2(a + b\left[\frac{W}{W_R} - 1\right] + cQ^2)\right) \qquad (2)$$

where k is the photon CM momentum, Λ is a universal cutoff factor, and the constants a, b, and c are searched for each multipole. The W-dependent term is included to account for any residual energy dependence, is purely phenomenological, and was found to significantly improve fits. Note that this term is constructed to given zero contribution both at the Q^2=0 (photoproduction) point and at the resonance position.

In Fig. 5, we compare the SAID and MAID results for electric and magnetic multipoles connected to the $\Delta(1232)$ resonance. At the resonance position, the R_{EM} ratio is essentially given by a ratio of the imaginary parts of these multipoles. The large magnetic multipole is not significantly different in these two analyses (the agreement is even closer for the SAID and DMT multipoles [7]). Differences for the electric multipole are much larger.

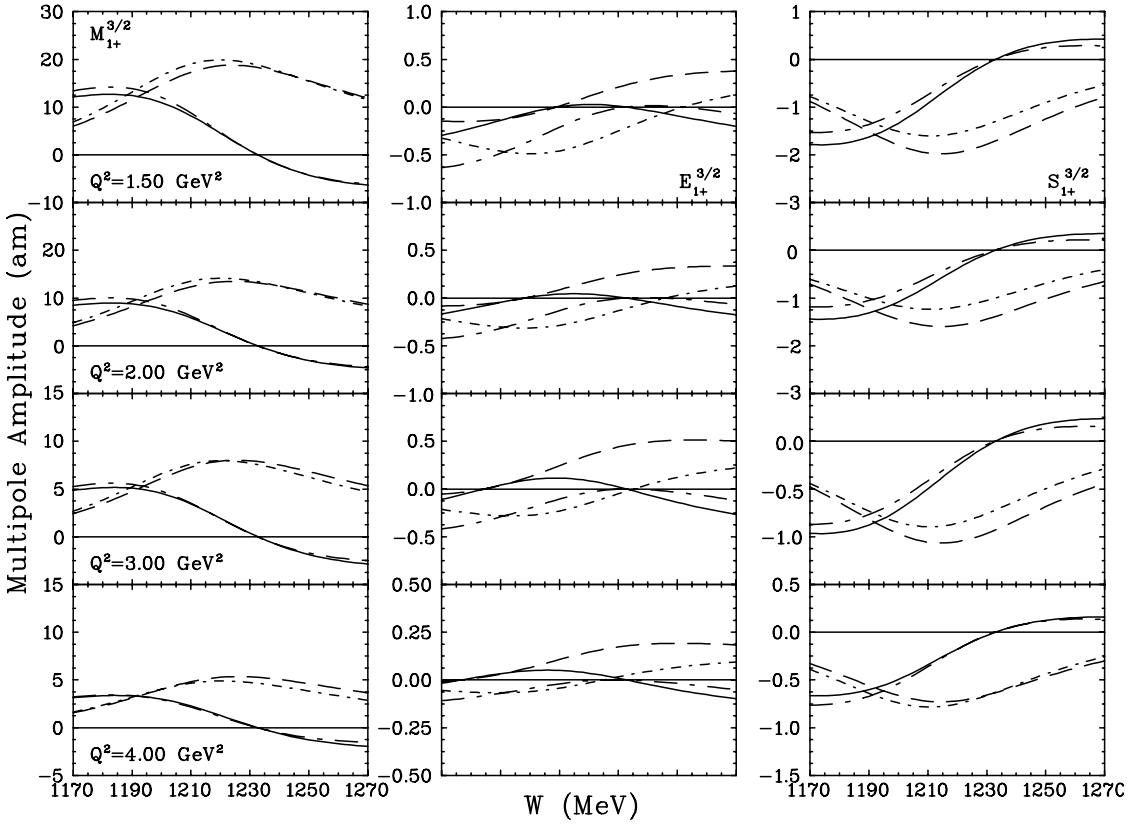

FIGURE 7. Magnetic, electric, and longitudinal P_{33} multipoles for $Q^2 > 1.00\ GeV^2$. Notation as in Fig. 5.

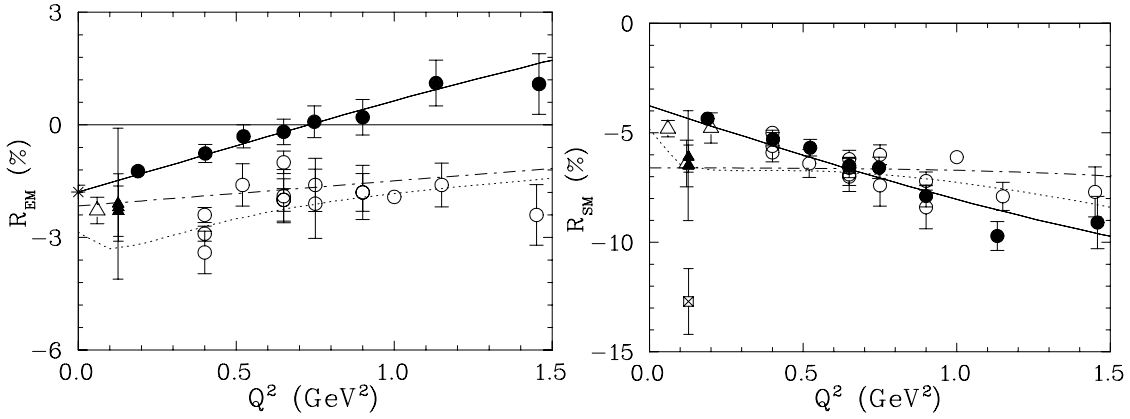

FIGURE 8. R_{EM} and R_{SM} ratios vs Q^2. Values were extracted from our fixed Q^2 analyses starting from the global fit (filled circles). Results from JLab [9] (open circles), MAMI-B [10] (open triangles), MIT-Bates [11] (filled triangles), and ELSA [12] (open square with cross) are given. At $Q^2 = 0$, $R_{EM} = -1.79 \pm 0.18$ % determined from pion photoproduction PWA [3] is shown (star). The solid curve gives our global (energy dependent) best-fit results. The long dash-dotted (MAID05) and dotted (DMT) curves are from Refs. [6, 7], respectively.

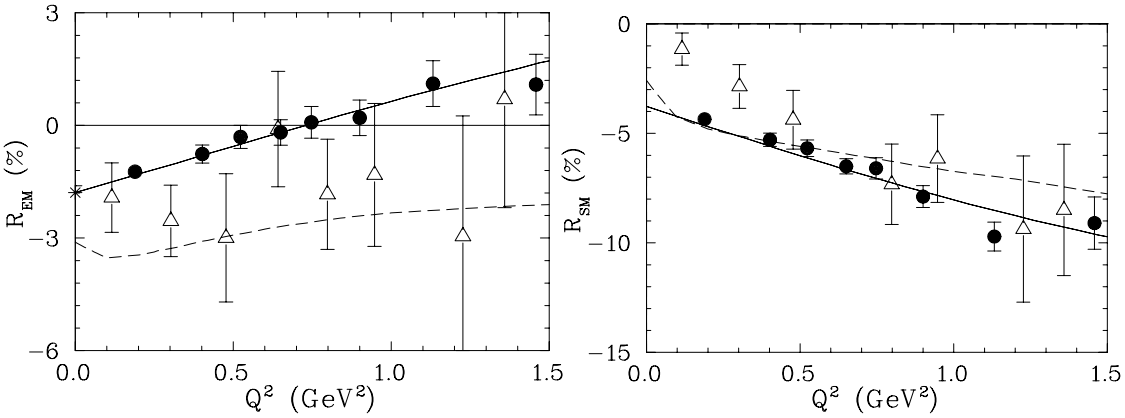

FIGURE 9. R_{EM} and R_{SM} ratios vs Q^2. Recent lattice [14] and previous S-L [13] calculations shown as open triangles and long dashed line, respectively.

In Figs. 6 and 7, we see the same trend continued for non-zero values of Q^2. At the resonance position, the magnetic ($M_{1+}^{3/2}$) multipoles remain fairly consistent; the $E_{1+}^{3/2}$ multipoles differ significantly.

One point of continuing interest has been the Q^2 variation of the ratio R_{EM} - a quantity which should tend to unity for suffiently high Q^2. In the SAID fits, a cross-over from negative to positive values of R_{EM} has been found, though the exact cross-over point has tended to shift as our database has expanded. The most recent results are shown in Fig. 8 compared to a number of models and single-Q^2 fits to data. Here, we also plot the ratio R_{SM}, for which there is at least qualitative agreement up to about 4 GeV^2. (The incorporation of high-Q^2 data is not complete, so there could yet be changes.) While our present curve for R_{EM} appears at odds with other determinations, it is not ruled out by recent lattice data [14], displayed in Fig. 9.

We plan to continue these fits, incorporating all available electroproduction data, and modifying our fitting procedure as necessary. Useful comparisons will require those involved in this effort to make available all amplitudes obtained in any new determination of R_{EM} and R_{SM}.

ACKNOWLEDGMENTS

This work was supported in part by the U. S. Department of Energy Grant DE–FG02–99ER41110 and by funding from Jefferson Laboratory.

REFERENCES

1. S. Eidelman *et al.*, *Review of Particle Physics*, *Phys. Lett. B* **592**, 1 (2004) and 2005 partial update for edition 2006; http://pdg.lbl.gov..
2. R.A. Arndt, W.J. Briscoe, I.I. Strakovsky, R.L. Workman, and M.M. Pavan, *Phys. Rev. C* **69**, 035213 (2004); R.A. Arndt, W.J. Briscoe, I.I. Strakovsky, and R.L. Workman, 'Extended

partial-wave analysis of πN scattering data', nucl-th/0605082.
3. R.A. Arndt, W.J. Briscoe, I.I. Strakovsky, and R.L. Workman, *Phys. Rev. C* **66**, 055213 (2004).
4. R.L. Workman, 'Single-channel fits and K-matrix constraints', nucl-th/0510025.
5. R. Koch, *Z. Phys. C* **29**, 597 (1985); G. Höhler, *Pion–Nucleon Scattering*, Landoldt–Börnstein Vol. **I/9b2**, edited by H. Schopper (Springer Verlag, 1983).
6. MAID05 version; D. Drechsel, O. Hanstein, S.S. Kamalov, and L. Tiator, *Nucl. Phys.* **A645**, 45 (1999).
7. S.S. Kamalov, Shin Nan Yang, D. Drechsel, O. Hanstein, and L. Tiator, *Phys. Rev. C* **64**, 032201 (2001).
8. I.G. Aznauryan, V.D. Burkert, H. Egiyan, K. Joo, R. Minehart, and L.C. Smith, *Phys. Rev. C* **71**, 015201 (2005).
9. V.V. Frolov *et al.*, *Phys. Rev. Lett. 82*, 45 (1999); K. Joo *et al.* (CLAS Collaboration), *Phys. Rev. Lett.* **88**, 122001 (2002); J.J. Kelly *et al.*, *Phys. Rev. Lett.* **95**, 102001 (2005); I.G. Aznauryan *et al.*, *Phys. Rev. C* **71**, 015201 (2005); M. Ungaro *et al.* (CLAS Collaboration), ' Measurement of the N to $\Delta(1232)$ transition at high momentum transfer by π^0 electroproduction', submitted to *Phys. Rev. Lett.*, hep–ex/0606042.
10. Th. Pospischil *et al.*, *Phys. Rev. Lett.* **86**, 2959 (2001); D. Elsner *et al.*, *Eur. Phys. J. A* **27**, 91 (2006); S. Stave *et al.*, 'Lowest Q^2 measurement of the $\gamma^* p \to \Delta$ reaction: probing the pionic contribution', nucl-ex/0604013.
11. C. Mertz *et al.*, *Phys. Rev. Lett.* **86**, 2963 (2001); C. Kunz *et al.*, *Phys. Lett. B* **564**, 21 (2003); N.F. Sparveris *et al.*, *Phys. Rev. Lett.* **94**, 022003 (2005).
12. F. Kalleicher *et al.*, *Z. Phys. A* **359**, 201 (1997).
13. T. Sato and T.S.H. Lee, *Phys. Rev. C* **54**, 2660 (1996).
14. C. Alexandrou *et al.*, *Phys. Rev. Lett.* **94**, 021601 (2005).